Active Site Coordination Chemistry of the Cytochrome *c* Peroxidase Asp235Ala Variant: Spectroscopic and Functional Characterization†

Juan C. Ferrer,‡ Paola Turano,§ Lucia Banci,*,§ Ivano Bertini,*,§ Ian K. Morris,∥ Kevin M. Smith,∥ Michael Smith,‡ and A. Grant Mauk*,‡

Department of Biochemistry and Molecular Biology, University of British Columbia, Vancouver, British Columbia V6T 1Z3, Canada, Department of Chemistry, University of California, Davis, California 95616, and Department of Chemistry, University of Florence, Florence, Italy

Received November 19, 1993; Revised Manuscript Received April 14, 1994®

ABSTRACT: Asp235 in yeast cytochrome *c* peroxidase forms a hydrogen bond with His175, the proximal histidyl residue, that has been suggested to be important in determining the electronic properties of the heme iron and that may be involved in stabilizing the higher oxidation states of the peroxidase that form transiently during catalysis. The current study employs ^1H and ^{15}N-NMR spectroscopy to study the electronic properties of and the effects of pH on the active site of the Asp235Ala variant. This variant exhibits three spectroscopic species between pH 5 and 9: a high-spin species that forms at low pH and two low-spin species that form successively at higher pH. Nevertheless, the activity of the variant exhibits a pH dependence virtually identical to that of the wild-type protein, though the activity of the variant is 3 orders of magnitude lower at all values of pH between pH 5 and 8.5. These findings suggest that the spin state and coordination environment of the heme iron in cytochrome *c* peroxidase do not dictate the rate of substrate (cytochrome *c*) oxidation. Binding of cyanide to the variant enzyme results in formation of a single species as detected by NMR spectroscopy. Analysis of high-resolution 1D and 2D ^1H-NMR and ^{15}N-NMR spectra of the cyanide adduct has permitted characterization of the properties of this derivative and the strength of the proximal ligand bond to the heme iron. Disruption of the hydrogen bond between the proximal histidine and Asp235 that exists in the wild-type enzyme dramatically reduces the strength of the interaction between the proximal ligand and the iron; this effect combined with concurrent changes in the distal heme-binding pocket accounts for the increase in reduction potential reported for the Fe^{3+}/Fe^{2+} couple. The catalytic consequences of the structural and electronic properties of the variant elucidated in this study are discussed.

The application of NMR spectroscopy to the investigation of paramagnetic metal centers and their environments in metalloproteins is well established as a powerful means of characterizing the structural and electronic properties of the active sites of these proteins (La Mar et al., 1973; Bertini & Luchinat, 1986; Bertini et al., 1993). Through correlating spectroscopic changes induced by mutations, ligand/substrate binding, and pH with the functional consequences of these factors, considerable insight can be gained concerning the mechanisms by which these proteins function. In previous work, paramagnetic NMR spectroscopy has been used in the study of several peroxidases (Thanabal et al., 1986, 1988; Satterlee & Erman, 1991; Satterlee et al., 1990, 1991; de Ropp et al., 1991; Banci et al., 1991a,b, 1992), heme proteins that catalyze the oxidation of a variety of organic substrates by hydrogen peroxide or organic peroxides. In such studies, cytochrome *c* peroxidase has been particularly important because until recently (Edwards et al., 1993; Piontek et al., 1993; Poulos et al., 1993) it has been the only peroxidase for which a three-dimensional structure has been reported (Finzel et al., 1984).

Yeast cytochrome *c* peroxidase (*Cc*P; EC 1.11.1.5)[1] is a monomeric mitochondrial heme protein (MW = 34 000) that catalyzes the oxidation of ferrocytochrome *c* by hydrogen peroxide (Bosshard & Yonetani, 1990). In the resting enzyme, the heme iron occurs in a pentacoordinated high-spin state (Dasgupta et al., 1989; Yonetani & Anni, 1987). *Cc*P reacts rapidly and stoichiometrically with hydrogen peroxide and other peroxides to form compound I, an intermediate form that is oxidized by two equivalents above the native ferric state of the enzyme (Jordi & Erman, 1974). Compound I possesses a ferryl iron center (Fe^{IV}=O) (Hager et al., 1972) and a radical center located at Trp191 (Sivaraja et al., 1989; Erman et al., 1989).

The three-dimensional structure of *Cc*P (Poulos et al., 1980; Finzel et al., 1984) established that the proximal and distal sides of the heme-binding pocket involve extensive hydrogen-bonding interactions (Figure 1). Six substitutions for Trp51 have been found to be hexacoordinate at neutral pH (Goodin et al., 1991), presumably through perturbation of these hydrogen-bonding interactions. On the proximal side of the heme-binding pocket, Asp235 plays a crucial role in determining the electronic properties of the iron and the catalytic properties of the enzyme through formation of hydrogen bonds with Trp191 and His175, the proximal heme iron ligand. The hydrogen-bonding interaction between Asp235 and Trp191 seems to be responsible for keeping this last residue in the optimal orientation, relative to the heme and His175 (Wang

† This research was supported in part by Medical Research Council of Canada Grant MT-7182 (to A.G.M.) and by National Institutes of Health Grant HL-22252 (to K.M.S.). The EPR spectrometer was purchased with funds provided by the Protein Engineering Network of Centres of Excellence.

‡ University of British Columbia.
§ University of Florence.
∥ University of California at Davis.

® Abstract published in *Advance ACS Abstracts,* May 15, 1994.

[1] Abbreviations: cytochrome *c* peroxidase, *Cc*P; lignin peroxidase, LiP; manganese peroxidase, MnP; horseradish peroxidase, HRP; human carbonic anhydrase, HCA.

0006-2960/94/0433-7819$04.50/0 © 1994 American Chemical Society

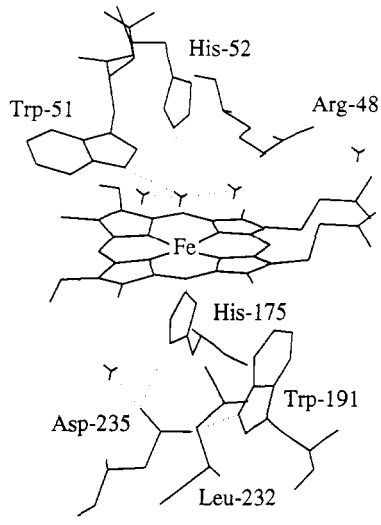

FIGURE 1: Active site of wild-type yeast cytochrome *c* peroxidase [from coordinates of Finzel et al. (1984)].

et al., 1990; Goodin & McRee, 1993), for the formation of the Trp191 radical in compound I. At the same time, the hydrogen bond between Asp235 and His175 endows the proximal heme ligand with marked histidinate character that manifests itself in two ways. First, the increased basicity of His175 leads to a strong interaction between this residue and the heme iron. This interaction keeps the iron ion ~0.2 Å out of the heme plane toward the axial ligand (Poulos et al., 1980; Finzel et al., 1984), and it is also responsible for a decreased affinity of the iron in the resting state for ligands in the sixth coordination site (Wang et al., 1990). Second, this property is thought to be important in the stabilization of the higher oxidation states of the iron that form transiently during the catalytic cycle of *Cc*P, though this possibility has recently been questioned (Vitello et al., 1992).

Crystallographic and resonance Raman studies of variants in which Asp235 has been replaced by Asn, Glu, and Ala have demonstrated that these substitutions produce significant structural changes that involve the hydrogen-bonding interactions on both sides of the heme prosthetic group (Smulevich et al., 1988, 1990, 1991; Wang et al., 1990; Satterlee et al., 1990; Goodin & McRee, 1993). Notably, the Asp235Asn variant is six coordinate and low spin at pH 6 (Smulevich et al., 1988; Satterlee et al., 1990); the iron atom in this enzyme moves toward the heme plane, and the distal water molecule (water595) resides within the iron coordination sphere (Wang et al., 1990). Similar changes have been suggested to occur in the Asp235Ala variant, though this protein has not yet been studied in similar spectroscopic detail or under as wide a range of solution conditions (Goodin & McRee, 1993).

In the current study, we have undertaken a detailed spectroscopic analysis of the Asp235Ala variant to assess the effects of removal of the Asp235His175 hydrogen bond on the structural, functional, and spectroscopic properties of cytochrome *c* peroxidase. The results establish that changes in the structure of the proximal heme-binding pocket of this enzyme can generate profound modifications in the organization of the distal heme environment and acute sensitivity to changes in pH and temperature.

EXPERIMENTAL PROCEDURES

Site-Directed Mutagenesis and Expression. The *Cc*P gene used in this work codes for the same number of amino acids as the mature sequence of the yeast protein, but the three amino terminal residues have been changed to MetLysThr (MKT) (Goodin et al., 1991). The two additional differences, Thr53Ile and Asp152Gly (Kaput et al., 1982), that the cloned *Cc*P gene possesses relative to the protein isolated from commercial yeast have been corrected (Fitzgerald et al., manuscript in preparation).

The system employed for the expression of *Cc*P(MKT) and the Asp235Ala variant in *Escherichia coli* (pT7*Cc*P(MKT)) derives from the pLACCCP2-9 plasmid (Goodin et al., 1990) in which the lac promoter has been replaced with the Φ-10a T7 phage promoter (Fitzgerald et al., manuscript in preparation). The Asp235Ala mutation was introduced oligonucleotide site-directed mutagenesis of single-stranded template DNA containing uracil, as previously described (Goodin et al., 1987). A 24-base oligonucleotide (5′-CTGCCCACTGCTTATTCTTTGATT-3′) synthesized with an Applied Biosystems 380A DNA synthesizer was used to convert the GAT (Asp) codon to GCT (Ala).

Protein Expression and Purification. In a typical preparation, eight 1-L cutures of *E. coli* BL21(DE3) (Studier et al., 1990) transformed with the pT7A235*Cc*P plasmid were grown at 37 °C for 12 h in a medium containing 10 g of bactotryptone, 8 g of yeast extract, 5 g of NaCl, 1 mL of glycerol, and 100 mg/L ampicillin. After 12 h, the expression of *Cc*P was induced by addition of 0.5 mM IPTG, and after 3 h, the cells were harvested by centrifugation. Subsequent steps were performed as described by Goodin et al. (1991). Approximately 25 mg of twice-recrystallized enzyme was obtained per liter of cell culture. Recombinant wild-type enzyme used for control experiments was produced from the same expression system and purified by the same procedure as described for the Asp235Ala variant.

Preparation of 8-CD_3-*Cc*P(MKT,A235) was performed by reconstituting the apoprotein with 8-(trideuteriomethyl)hemin by standard methods used for reconstitution with protoheme IX (Yonetani, 1967; Fishel et al., 1987). The 8-(trideuteriomethyl)protoheme IX was synthesized as described by Smith et al. (1986); the sample used in this work was determined by ^{1}H-NMR spectroscopy to be ~30% enriched in deuterium. Dε1-His *Cc*P(MKT,A235) was prepared by growing eight 1-L cultures of *E. coli* BL21(DE3) containing the mutant pT7A235*Cc*P plasmid in M9 minimal salt medium with 0.2% glucose and supplemented with 0.1 mM $CaCl_2$, 1 mM $MgSO_4$, 50 mg/L thiamin, 50 mg/L biotin, and 100 mg/L concentrations of all the L-amino acids except histidine (Hibler et al., 1987). After 12 h at 37 °C, 200 mg/L Dε1-His was added and the production of the isotopically labeled enzyme was induced 15 min later by addition of 0.5 mM of IPTG. After 3 h at 37 °C, the cells were harvested by centrifugation and the enzyme was isolated as described above.

Electronic Spectroscopy. Electronic spectra were obtained at 298 K, unless otherwise stated, with a Cary 219 spectrophotometer fitted with a circulating water bath and interfaced to a microcomputer (On-Line-Instrument-Systems, Bogart, GA). The extinction coefficients of *Cc*P(MKT,A235) in various buffers were determined by the pyridine hemochromogen method (De Duve, 1948). The spectrophotometric pH titrations were performed by dissolving the protein (ca. 10 μM) in 0.1 M potassium phosphate or 10 mM potassium phosphate/250 mM potassium nitrate buffer (2 mL) and adjusting the pH with a concentrated solution of potassium hydroxide.

Kinetic Measurements. Yeast iso-1-cytochrome *c* was isolated and purified as described previously (Rafferty et al., 1990). Cytochrome *c* concentration was determined on the

basis of a molar absorptivity of the Fe(II) protein at 550 nm (29.0 mM^{-1} cm^{-1}) (Margoliash & Frohwirt, 1959) or from the reduced minus oxidized spectrum of cytochrome c, assuming a difference in molar absorptivity of 21.2 mM^{-1} cm^{-1} at 550 nm (Yonetani & Ray, 1965). Hydrogen peroxide was standardized by titration with potassium permanganate (Kolthoff & Belcher, 1957).

Steady-state rates of the CcP-catalyzed oxidation of yeast ferrocytochrome c by H_2O_2 were determined as described by Kang and Erman (1982) and were carried out at 298 K (10 mM potassium phosphate/250 mM potassium nitrate buffer). Kinetic measurements were performed by mixing ferrocytochrome c (30 μM, >95% reduced), H_2O_2 (170 μM), and the enzyme (0.5 μM). Steady-state rate constants are reported as turnover numbers (V_o/e).

EPR Spectroscopy. EPR spectra were collected in 4-mm quartz tubes at X-band with a Bruker ESP300E spectrometer (100-kHz field modulation). The instrument was equipped with an Oxford Instruments ESR900 liquid helium cryostat and an ITC4 temperature controller.

NMR Spectroscopy. ^{1}H-NMR spectra of CcP(MKT), CcP(MKT,A235), and their cyanide derivatives (~2 mM in 0.1 M sodium phosphate) were recorded with Bruker MSL 200 and AMX 600 spectrometers. The pH of protein samples prepared for NMR spectroscopy was measured (uncorrected for the isotope effect) with an Orion Model 720 pH meter and a Microelectrodes Inc. Model MI-410 microcombination pH probe. T_1 experiments were performed at 200 MHz with the MODEFT (modified driven equilibrium Fourier transform) pulse sequence (Hochman & Kellerhalls, 1980), by varying the delay time between subsequent pulses from 512 to 1 ms and using a recycle delay of 512 ms. The resulting data have been fitted to a single-exponential decay. The estimated error of the resulting T_1 values is ±15%. All other spectra at 200-MHz resolution were obtained using a superWEFT (water-eliminated Fourier transform) pulse sequence (Inubushi & Becker, 1983) with a recycle delay of 120 and 200 ms for the native and cyanide-inhibited species, respectively. The identification of the two nonexchangeable protons of the proximal histidine ring in the cyanide adduct of CcP-(MKT,A235) was obtained by a superWEFT pulse sequence with a recycle delay of 10 ms and a τ value of 5 ms. The nuclear Overhauser effect (NOE) difference spectra were collected as described previously (Banci et al., 1989). $KC^{15}N$ (>99% enrichment) was obtained from Isotec and used without further purification. The ^{15}N-NMR spectra were recorded with a Bruker AMX 600 spectrometer with a modification of a pulse sequence designed to reduce the effects of the dead time (Belton et al., 1985). The spectra were collected with a recycle delay of 100 ms and about 900 000 scans.

NOESY and COSY spectra in H_2O were recorded at 600 MHz using presaturation to eliminate the water signal. Phase-sensitive (TPPI) NOESY spectra (Macura et al., 1982; Marion & Wüthrich, 1983) (289 and 294 K) were recorded at mixing times of 15 ms to avoid spin diffusion. Spectra (512) were collected with 1K data points in the F2 direction. The data were multiplied in both dimensions by a sine-squared bell window function with a phase shift of 45° and zero-filled to obtain 1K × 1K real data points. According to previous results (Yu et al., 1990; Bertini et al., 1991), magnitude-type COSY experiments (Aue at al., 1976) were performed to detect scalar connectivities between the paramagnetic shifted signals. COSY spectra consisting of 512 experiments with 1K data points in the F2 direction were processed in both dimensions by a pure sine-squared bell window function and zero-filled to obtain 1K × 1K real data points.

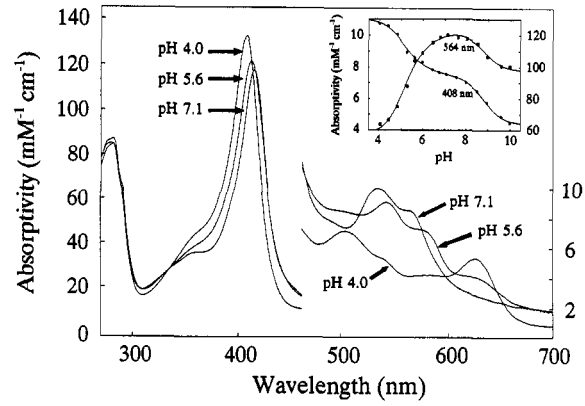

FIGURE 2: Electronic spectra of Asp235Ala-CcP in 100 mM phosphate buffer (298 K) at selected pH. Inset: spectrophotometric pH titration monitored at two wavelengths, 564 nm (squares, left axis) and 408 nm (circles, right axis). The solid lines represent the nonlinear fit of these data to three single-proton processes with apparent pK_a of 5.1 ± 0.3, 6.5 ± 0.2, and 8.8 ± 0.2.

RESULTS

Electronic Spectroscopy. Three pH-dependent forms of the protein are observed between pH 4 and 9 in 0.1 M potassium phosphate buffer (Figure 2). At low pH, the predominant species exhibits an electronic spectrum indicative of a six-coordinate high-spin Fe(III) derivative (HS; λ_{max} = 408, 501, 626 nm). As the pH is increased at 298 K, a new species appears (pK_a = 5.1 ± 0.3) that has a spectrum characteristic of a six-coordinate, low-spin derivative (LS1; λ_{max} = 414, 543, 578 nm). Increasing the pH further generates (pK_a = 6.5 ± 0.2) a third component that exhibits an electronic spectrum consistent with the formation of a second six-coordinate, low-spin derivative (LS2; λ_{max} = 415, 533, 564 nm). Finally, at higher pH, the enzyme denatures with an apparent pK_a of 8.8 ± 0.2. The absorbance of the variant as monitored at two wavelengths is illustrated in Figure 2 (inset), and the pK_a values indicated were determined from the nonlinear least-squares fits to the data shown in this figure. In 10 mM potassium phosphate/250 mM potassium nitrate buffer, the variant enzyme also exhibits four pH-dependent forms between pH 4 and 9. The apparent pK_a values are 4.2 ± 0.2 for the HS to LS1 transition, 5.8 ± 0.2 for the LS1 to LS2 transition, and 8.3 ± 0.3 for the denaturation of the enzyme.

The electronic spectrum of the Asp235Ala variant is markedly temperature dependent. At pH 6.15 in 0.1 M potassium phosphate buffer or at pH 6.00 in 10 mM potassium phosphate/250 mM potassium nitrate buffer, the predominant spectroscopic species present at 282 K is LS1. On warming the sample to 309 K, the nearly quantitative conversion to the LS2 derivative results in both buffers, and the LS1 ⇄ LS2 equilibrium is fully reversible. This finding suggests that the pK_a for the LS1 ⇄ LS2 equilibrium is highly sensitive to changes in temperature.

Steady-State Kinetics. The catalytic activity of the Asp235Ala variant is approximately 3 orders of magnitude lower than that of the wild-type enzyme between pH 4.8 and 8.55 and is strongly dependent on pH over the range studied (Figure 3).

EPR Spectroscopy. The EPR spectrum (5 K) of the Asp235Ala variant at pH 7 is shown in Figure 4A. This spectrum is characteristic of a six-coordinate, high-spin iron

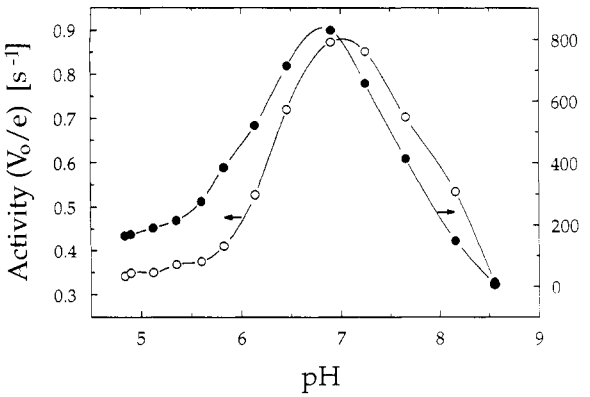

FIGURE 3: Steady-state activity as a function of pH for the oxidation of yeast iso-1-ferrocytochrome *c* by wild-type *Cc*P (solid circles, right axis) and the Asp235Ala variant (open circles, left axis). Conditions: 10 mM potassium phosphate buffer in the presence of 250 mM potassium nitrate (25 °C).

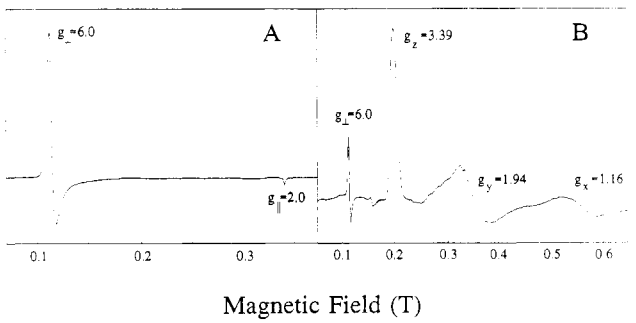

FIGURE 4: EPR spectra of the Asp235Ala variant (5 K) in the absence (A) and presence (B) of 10 equiv of potassium cyanide.

system with axial symmetry. As the electronic spectrum of this protein in the same buffer (298 K) is that of a six-coordinate, low-spin heme iron, it is apparent that this variant experiences a transition to a high-spin species at cryogenic temperatures, thereby restricting the usefulness of EPR spectroscopy in understanding the behavior of this variant at room temperature. The EPR spectrum of the variant in the presence of 10 equiv of potassium cyanide (Figure 4B) indicates the presence of a mixture of low-spin (cyanide-bound) and high-spin (g = 6) (cyanide-free) components. For the low-spin component, g_z = 3.39, g_y = 1.94, and g_x = 1.16 are measured. These g values indicate that the cyanide adduct of the wild-type enzyme is less anisotropic [i.e., g_z = 3.0, g_y = 2.1, and g_x = 1.2 (Blumberg et al., 1968; Wittenberg et al., 1968)] as is the cyanide adduct of myoglobin [i.e., g_x = 3.45, g_y = 1.89, and g_x = 0.93 (Hori, 1971)]. Both the NMR and electronic spectra of this sample indicated that the variant enzyme was completely converted to the cyanide-bound form at room temperature under these conditions.

NMR Spectroscopy of the Native Asp235Ala Variant. Figure 5A,B shows the NMR spectra of wild-type *CcP* and the Asp235Ala variant at 294 K in 0.1 M phosphate buffer, pH 6.5. Unlike the spectra of the wild-type enzyme and other peroxidases (Satterlee et al., 1983; Thanabal et al., 1986, 1988; Banci at al., 1991b, 1992; de Ropp et al., 1991), the chemical shifts of this variant are much less shifted and occur in the 40 to −5 ppm region. The spectrum shows two signals (the two shifted farthest downfield) of greater intensity than the others. These signals are probably attributable to the heme methyl groups because the signals assigned to the heme methyl groups in other low-spin iron (III) heme proteins are similarly intense and shifted farther downfield than the other resonances observed. Other signals with lower intensity which

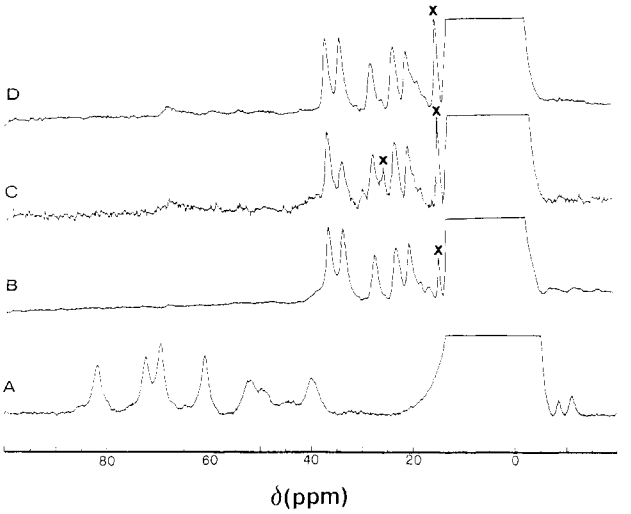

FIGURE 5: 200-MHz, ^{1}H-NMR spectra (294 K, pH 6.5, 0.1 M phosphate buffer, 100% H_2O) of (A) native wild-type *Cc*P, (B) native Asp235Ala variant, (C) 8-(trideuteriomethyl)protoheme IX-substituted variant, and (D) Dϵ1-His-Asp235Ala-labeled Asp235Ala-*Cc*P variant. Signals labeled X arise from impurities.

could represent single-proton resonances of the other heme substituents are also observed.

The ^{1}H-NMR spectrum of the variant is highly pH dependent (Figure 6). At pH 4.5 (the lowest pH at which the protein is stable at the concentration required for NMR measurements), this variant shows downfield-shifted resonances in the 70–35 ppm range (Figure 6A) together with signals of the species present at neutral pH. These chemical shift values suggest the presence of a high-spin heme iron species (HS). The spectrum of HS is characterized by the heme methyl signals in the 63–50 ppm region and by some single-proton signals at ~40–30 ppm. A broad signal is detected at 70.5 ppm, which is the resonance that is shifted the furthest downfield. In other peroxidases, an exchangeable signal observed in the 90–80 ppm range has been assigned as the NHδ1 proton of the proximal histidine. The NHδ1 proton has been reported to exchange slowly with D_2O in some peroxidases, owing to an unfavorable exchange rate with the solvent. Therefore, it is possible that the broad signal at 70.5 ppm in the present system arises from the NHδ1 proton of the proximal histidine.

As the pH is raised from 4.5 toward neutrality, the chemical shifts of the resonances attributable to the high-spin species increase and their intensities decrease. This observation indicates that under these conditions, HS is in equilibrium with two species, one of which is fast and the other of which is slow on the NMR time scale. At pH 6, the resonances of HS disappear, and between pH 6.0 and 6.7, only a low-spin species (LS1) is present (Figure 6C,D). The formation of LS1, the species in slow equilibrium with HS, occurs with pK_a ~ 5. From the shift differences of the heme methyl signals in the spectrum obtained at pH 4.5 with respect to those in the spectrum at neutral pH, an upper limit of 2.4 × 10^4 s^{-1} can be estimated for the exchange rate between HS and LS1. This slow rate is consistent with the occurrence of a significant conformational change (see Discussion). An equilibrium between high-spin and low-spin forms has also been reported for the Asp235Asn variant that is analogous to the HS ⇌ LS1 equilibrium (Satterlee et al., 1990). At pH values higher than 7, another low-spin species (LS2) appears with the concomitant disappearance of LS1 (Figure 6E,F). The formation of LS2 occurs with pK_a ~ 7. As found for HS and

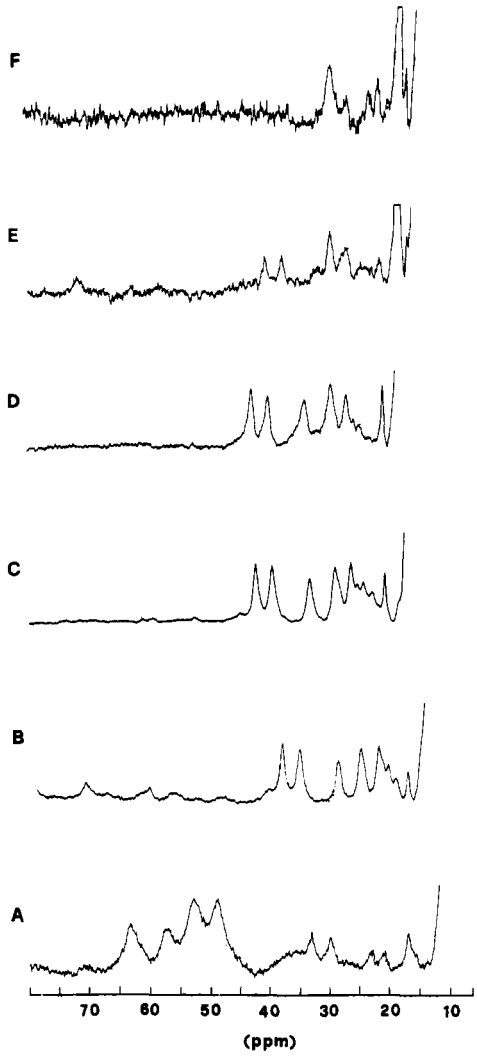

FIGURE 6: 200-MHz ^{1}H-NMR spectra of the Asp235 variant (100 mM sodium phosphate buffer, 100% H_2O, 296 K): (A) pH 4.5, (B) pH 5.3, (C) pH 6.0, (D) pH 6.7, (E) pH 7.2, and (F) pH 8.2.

LS1, the interconversion between LS1 and LS2 occurs at a relatively slow rate (1×10^4 s^{-1}), as expected for a significant structural rearrangement. As the pH is raised above 8, the sample denatures.

The temperature dependence of the NMR resonances has been studied between 281 and 311 K at pH 6.1. In this temperature range, the LS1 resonances exhibit anti-Curie behavior (Figure 7A–G), suggesting either fast exchange on the NMR time scale between two species (one with $S = {}^1/_2$ and the other with higher S values of ${}^5/_2$ or ${}^3/_2$) or the presence of a spin admixture. In the case of fast exchange, the equilibrium should occur between LS1 and a species different from HS because we know that HS and LS1 are in slow exchange on the NMR time scale. By further increasing the temperature, LS1 converts to the LS2 species (Figure 7H), consistent with a decrease in the value of the second pK_a of about 1 pK unit on increasing the temperature from 296 to 310 K. The thermal interconversion of LS1 and LS2 is completely reversible with no evidence of protein denaturation.

Figure 5C shows the spectrum of the 8-(trideuteriomethyl)-heme-substituted derivative of the Asp235Ala variant. By comparison with the spectrum shown in Figure 5B, it appears that the intensity of one of the heme methyl signals (at 33 ppm) is greatly reduced in the 8-(trideuteriomethyl)heme-substituted derivative (the residual signal observed is attributed to incomplete deuteration); therefore, this signal is assigned

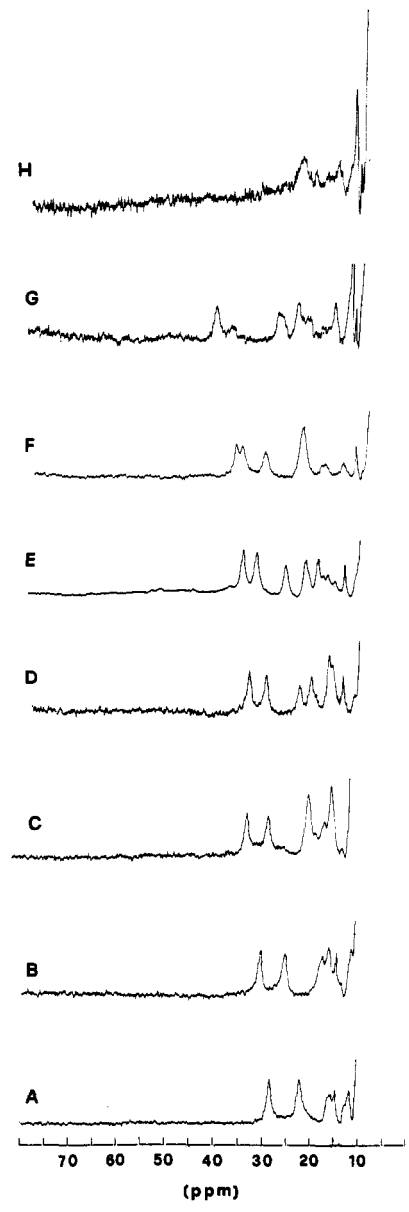

FIGURE 7: 200-MHz ^{1}H-NMR spectra of the Asp235Ala variant (100 mM sodium phosphate buffer, 100% H_2O, pH 6.1): (A) 282 K, (B) 287 K, (C) 291 K, (D) 293 K, (E) 296 K, (F) 301 K, (G) 306 K, and (H) 310.5 K.

to the 8-CH_3 group. No paramagnetically shifted signals disappeared when the spectrum of the sample prepared with deuterated histidine at Hϵ1 was recorded (Figure 5D), and no signal disappeared when the spectrum of the enzyme exchanged into D_2O was recorded. The Hϵ1 resonance of the proximal His is not observed in the spectrum of the Asp235Ala variant, despite the significant low-spin character of this protein at this pH (pH 6.5). Indeed, in the low-spin forms of other peroxidases or globins, this resonance is found to be shifted outside the diamagnetic envelope. Unfortunately, instability of the variant enzyme at high concentrations prevented characterization of LS1 and LS2 by 2D NMR methods.

NMR Spectroscopy of the Cyanide Adduct. The CN^--bound form of the Asp235Ala variant is in slow exchange with the unligated form on the time scale of the ^{1}H-NMR measurement. The spectrum of the cyanide adduct is that of a single species with hyperfine shifts typical for a low-spin iron (III) moiety. Figure 8A shows the 200-MHz ^{1}H-NMR spectrum of Asp235Ala-CN^- recorded in H_2O at 294 K. Downfield, there are two signals with an estimated relative

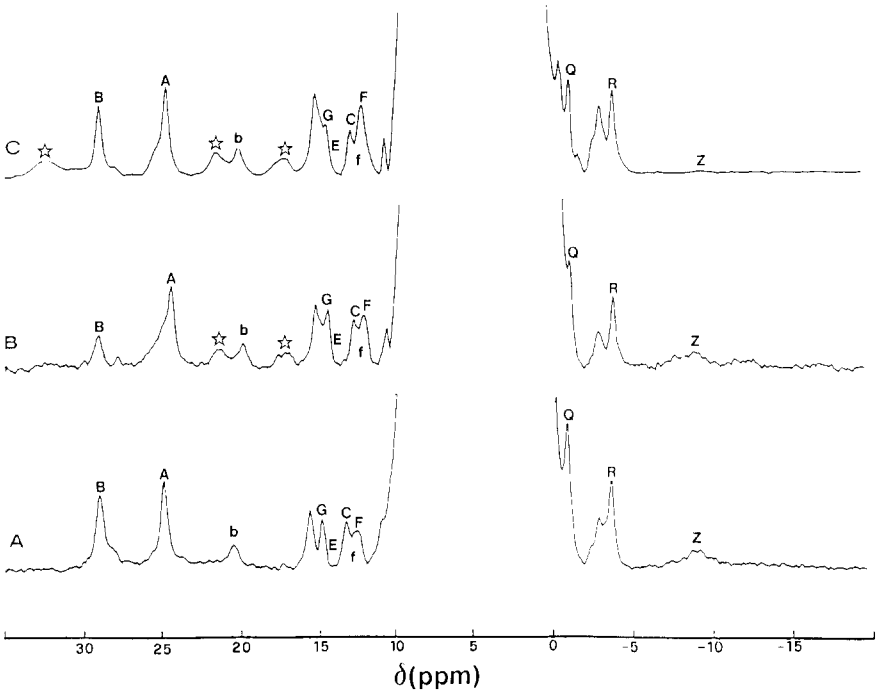

FIGURE 8: 200-MHz ^{1}H-NMR spectra (294 K) of the cyanide adducts of (A) Asp235Ala, (B) 8-(trideuteriomethyl)protoheme IX-substituted Asp235Ala variant, and (C) Dε1-His-Asp235Ala. Each protein sample was in 0.1 M sodium phosphate buffer (90% H_2O/10% D_2O, pH 7). Resonances attributable to impurities are indicated with a star.

intensity indicative of three protons that are attributable to heme methyl groups, and there are several additional single-proton resonances. Four of the resolved signals arise from exchangeable protons. The resolved upfield portion of the spectrum exhibits two three-proton signals, some single-proton signals, and a broad resonance at about −10 ppm. The chemical shifts and T_1 values observed in this spectrum are set out in Table 1 along with those reported previously for the CN^- adducts of other *Cc*P derivatives for purposes of comparison. In this table and in the spectra, lowercase letters are used to designate exchangeable protons.

In contrast to other peroxidases, the 2-vinyl group in *Cc*P is oriented so that none of its protons exhibits significant dipolar coupling with the 3-CH_3 group. This fact prevents us from making the assignment of the individual methyl groups directly; so, to overcome this difficulty, we studied the 8-(trideuteriomethyl)protoheme IX-reconstituted variant. The spectra obtained for the cyanide adduct of the 8-(trideuteriomethyl)protoheme IX-substituted peroxidase and for the Dε1-His peroxidase samples are reported in Figure 8B,C, respectively. Comparison of the spectra reported in Figure 8 permits assignment of signal B as 8-CH_3 and signals G and Z as Hε1 of the distal and proximal histidines, respectively. As observed for other low-spin Fe(III) heme proteins (Bertini & Luchinat, 1986; Satterlee at al., 1983; de Ropp et al., 1984, 1991; Banci et al., 1991a,b, 1992), the NMR signals of the heme CH_3 groups are found to be shifted in a pairwise fashion such that the two CH_3 groups 180° apart from each other experience similar chemical shifts. This pattern has been rationalized on the basis of π spin delocalization on the heme ring (Shulman et al., 1971; La Mar & Walker, 1979; Thanabal et al., 1987a). In the spectra of the CN^- adducts of wild-type *Cc*P and other peroxidases, the 8-CH_3 and 3-CH_3 resonances are invariably shifted downfield while the 5-CH_3 and 1-CH_3 resonances fall in the diamagnetic envelope (Satterlee et al., 1983; de Ropp et al., 1984, 1991; Banci et al., 1991a,b, 1992). This well-established pattern makes us confident in assigning signal A to the 3-CH_3 group.

Table 1: Chemical Shift and 200-MHz Nonselective T_1 Values Observed for the Hyperfine Shifted Resonances for the Cyanide Derivatives of Asp235Ala at 294 K, WT at 301 K, and Asp235Asn at 294 K[a]

assignment	Asp235Ala shift (ppm)	T_1[d] (ms)	WT[b] shift (ppm)	T_1 (ms)	Asp235Asn[c] shift (ppm)	signal
2-Hα	8.7[e]	*f*	7.1[g]	*f*		J
2-$H\beta_{cis}$	−4.1[e]	*f*	−3.7[g]	*f*		X
2-$H\beta_{trans}$	−3–3[e]	*f*	−3.0[g]	*f*		Y
3-CH_3	24.0	41	30.6	39	27.4	A
4-Hα	13.8	*f*	16.5	*f*	15.2	E
4-$H\beta_{trans}$	−1.9[e]	*f*	−2.1[g]	*f*		V
4-$H\beta_{cis}$	−3.7[e]	*f*	−3.8[g]	*f*	−3.8	W
7-Hα	10.5[e]	*f*	18.5	43	17.7	D
7-Hα′	6.2[e]	*f*	6.4[g]	*f*		I
7-Hβ	−1.8[e]	*f*	−1.3[g]	*f*	−1.4	M
7-Hβ′	3.0[e]	*f*	3.0[g]	*f*		N
8-CH_3	28.2	24	28.1	40	26.3	B
NHp prox His			13.0	140	12.8	d
Hα prox His	7.6[e]	*f*				J′
Hβ prox His	12.3	47	19.6	29	19.5	C
Hβ′ prox His	11.4	24	14.9	35	13.9	F
Hδ1 prox His	11.8[h]	*f*	10.1[h]	*f*		f
Hε1 prox His	−9.7	≤3	−22.2	2.6	−15.8	Z
Hδ2 prox His		≤3	17.6	≤3		H′
Hδ1 dist His	16.3		16.8[h]	*f*		c
Hε1 dist His	13.9	52	13.9	69	13.6	G
Hδ2 dist His	8.7[e]	*f*				H
Hε2 dist His	27.1	∼3	29.0	*f*		a
Hγ Leu232	−0.4[e]	*f*	0.7[g]	*f*		P
δ′-CH_3 Leu232	−1.8[e]	*f*	−1.1[g]	*f*		Q
δ-CH_3 Leu232	−4.5[e]	50	−2.8[g]	*f*		R

[a] Lowercase letter labeling corresponds to exchangeable protons. [b] Taken from Banci et al. (1991a). [c] Taken from Satterlee et al. (1990). [d] The error on T_1 values is about 15%. [e] The shift value was measured from 2D maps obtained at 600 MHz and 294 K. [f] Not measured because the signal is in a complex envelope. [g] The shift value was measured from 2D maps obtained at 600 MHz and 298 K (Banci et al., 1991a). [h] The shift value was measured in NOE difference spectra.

The assignment of the remaining resonances in the spectrum of the cyanide adduct has been performed mainly on the basis of NOESY experiments at 600 MHz. In Figure 9, the

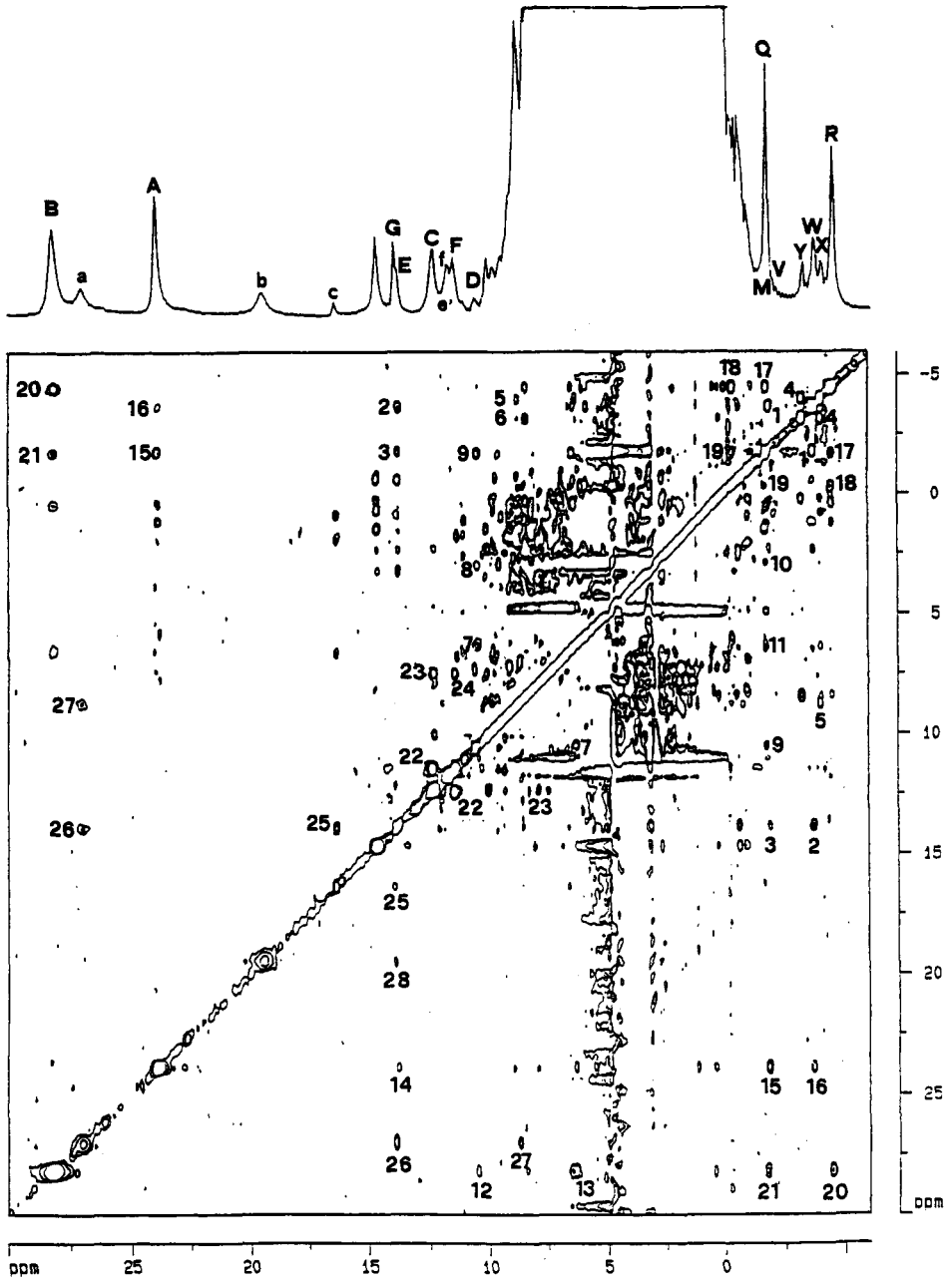

FIGURE 9: 600-MHz NOESY spectrum (294 K, 0.1 M sodium phosphate buffer, 90% H_2O/10% D_2O, pH 7) of the cyanide adduct of the Asp235Ala variant in water obtained with a 15-ms mixing time. Cross-peak assignments are as follows: (1) 4-Hβ_{cis}, 4-Hβ_{trans}; (2) 4-Hα, 4-Hβ_{cis}; (3) 4-Hα, 4-Hβ_{trans}; (4) 2-Hβ_{cis}, 2-Hβ_{trans}; (5) 2-Hα, 2-Hβ_{cis}; (6) 2-Hα, 2-Hβ_{trans}; (7) 7-Hα, 7-Hα'; (8) 7 -Hα, 7-Hβ'; (9) 7-Hα, 7-Hβ; (10) 7-Hβ, 7-Hβ'; (11) 7-Hα', 7-Hβ; (12) 8-CH_3, 7-Hα; (13) 8-CH_3, 7-Hα'; (14) 3-CH_3, 4-Hα; (15) 3-CH_3, 4-Hβ_{trans}; (16) 3-CH_3, 4-Hβ_{cis}; (17) δ'-CH_3 Leu232, δ-CH_3 Leu232; (18) Hγ Leu232, δ-CH_3 Leu232; (19) Hγ Leu232, δ'-CH_3 Leu232; (20) 8-CH_3, δ-CH_3 Leu232; (21) 8-CH_3, δ'-CH_3 Leu232; (22) Hβ His175; Hβ' His175; (23) Hβ His175, Hα His175; (24) Hβ' His175, Hα His175; (25) Hδ1 His52, Hϵ1 His52; (26) Hϵ2 His52, Hϵ1 His52; (27) Hϵ2 His52, Hδ2 His52; (28) NH proton of Arg48 (b), Hϵ1 His52; (29) NH proton of Arg48 (b), NH proton of Arg48 (e'). Cross-peak 29 becomes evident only with use of a different set of processing parameters, owing to the large line width of signals b and e'. The 1D 600-MHz ^{1}H-NMR spectrum is also reported.

NOESY spectrum obtained in H_2O at 600 MHz and 294 K is reported. Assignment of the cross-peaks is reported in the caption to Figure 9. All the NOESY connectivities observed in Figure 9 are confirmed by a NOESY experiment performed at 289 K. The assignments resulting from 2D and 1D (see below) experiments are summarized in Table 1.

Having assigned signal B as 8-CH_3 allows us to assign signal D as 7-Hα. The latter signal exhibits NOESY connectivities with signals I, M, and N, and it is coupled in a scalar fashion with I. This NOESY connectivity pattern suggests that I, M, and N arise from 7-Hα', 7-Hβ', and 7-Hβ protons, respectively. Signal A, a CH_3 group, exhibits dipolar coupling with signals E, V, and W, which in turn exhibit both dipolar and scalar coupling characteristic of a vinyl group. This pattern and the considerations indicated above concerning the shift of the heme methyl groups in low-spin derivatives of peroxidases establish that resonance A is attributable to the 3-CH_3 group and that E, V, and W represent the Hα, Hβ_{trans}, and Hβ_{cis} protons of the 4-vinyl group. NOESY and COSY patterns similar to those observed among signals E, V, and W are also observed among signals J, X, and Y, thus allowing us to assign the latter signals to the Hα, Hβ_{trans}, and Hβ_{cis} protons of the 2-vinyl group, respectively. Cross-peaks in COSY maps can be present even in the absence of scalar coupling if strong proton–proton dipolar coupling (i.e., short proton–proton distances) is operative and if the proton signals are broad

(Bertini et al., 1993b). This situation may be the case for the geminal Hβ protons of the heme vinyl substituents. For the Hβ–Hα pairs of these groups, both the dipolar coupling and the line widths are too small to produce these effects (Banci et al., in press).

Among the other downfield-shifted signals, an intense NOESY cross-peak is observed between signals C and F, suggesting that they originate from geminal protons. On the basis of this feature and their chemical shift values, we assign these resonances to the Hβ protons of proximal histidine His175. Signals C and F both exhibit a NOESY cross-peak with signal L, which permits the assignment of L to the Hα proton of the same histidine. The upfield signal Z has been assigned to the Hε1 of a histidine ring through selective deuteration. The similarity in the pattern of chemical shifts observed for wild-type CcP and for other peroxidases (La Mar et al., 1982; Satterlee et al., 1983; Banci et al., 1991b, 1992) allows us to assign this signal as arising from the Hε1 proton of His175. The availability of the Dε1-His sample confirms this conclusion and permits the first unambiguous assignment of this proximal histidine resonance (Z) to the Hε1 proton. Singal Z is too broad to be detected in the 2D maps obtained at 600 MHz. However, its saturation at 200 MHz provides an NOE with the exchangeable proton f, which permits its assignment to the Hδ1 proton of the proximal histidine. Finally, by collecting the spectrum with a very fast repetition rate to saturate all the relatively slow relaxing signals, a broad signal (H′) can be detected at 14.6 ppm ($T_1 \sim 3$ ms). On the basis of this property and on similarity with the spectra of other peroxidases (Thanabal et al., 1987a,b; Banci et al. 1991ab, 1992), we assign signal H′ to the Hδ2 proton of His175.

In the downfield region, other exchangeable signals are present. Signal a gives a NOESY cross-peak with signal G. On the basis of the results obtained with the Dε1-His derivative, signal G can be attributed to Hε1 of the distal histidine (His52) and signal a as Hε2 of the same residue. Signal G exhibits strong NOESY connectivity with signal c, which has a very low intensity (the result of saturation transfer from bulk water). Signal c is due to the Hδ1 of the distal histidine. Signal a also exhibits dipolar connectivity with a signal at 8.7 ppm which is probably Hδ2 of the distal His. As in the spectrum of the wild-type protein, signal b is attributable to another residue in the distal heme pocket, probably Arg48. This resonance exhibits dipolar connvectivity with signal G and with a signal at 12.1 ppm, which by analogy with wild-type CcP (Banci et al., 1991a) can be labeled as e′.

In the upfield region of the spectrum, the resonances Q and R are coupled in a dipolar manner to each other, and both show NOESY (and COSY) cross-peaks with signal P. This pattern of connectivities could indicate that Q and R arise from the two CH_3 groups of a Leu or Val residue and that P is the proton of the vicinal CH group. Analogously to wild-type CcP, the 8-CH_3 signal shows NOESY cross-peaks with the two CH_3 signals of this residue, thus permitting identification of this residue as Leu232 because there is no valine adjacent to the heme. COSY cross-peaks between the $CH_3\delta$–$CH\gamma$ and $CH_3\delta'$–$CH\gamma$ couplings in Leu232 are detecting real scalar coupling arising from the properties of the proton signals, as discussed above for the heme vinyl protons.

The ^{15}N-NMR spectra of the cyanide adducts of the wild-type enzyme and the Asp235Ala variant exhibit a broad signal at 587 and 689 ppm, respectively, that is similar to those reported previously for other peroxidases (Banci et al., 1993). It has been proposed previously (Golding et al., 1976; Morishima & Inubushi, 1978) and reported for several systems (Behere et al., 1985; Banci et al., in press; Morishima et al., 1977; Morishima & Inubushi, 1977, 1978; Shiro et al., 1989) that the value of this chemical shift is directly related to the strength of the axial ligand–iron bond.

DISCUSSION

The substitution of the negatively charged Asp235 residue in CcP with a neutral hydrophobic residue, Ala, profoundly alters the coordination chemistry of the heme iron by modifying the electrostatic properties of the active site. The three-dimensional structure of the Asp235Ala-CcP variant (Goodin & McRee, 1993) establishes that this substitution results in structural reorientation of Trp191 in the proximal heme-binding pocket, but it could not be established whether or not a water molecule is bound as the sixth ligand. As the properties of this variant and the closely related Asp235Asn variant are strongly dependent on pH, additional studies were required to gain further insight into the behavior of these variants.

pH Dependence of the Asp235Ala-CcP Coordination Environment. Analysis of the pH and temperature dependencies of the electronic spectrum and of the paramagnetically shifted signals in the ^{1}H NMR spectrum of the Fe(III)-Asp235Ala variant allows identification of three spectroscopically distinct forms of this enzyme as well as the denatured enzyme that forms at very high pH. At low pH, the electronic and ^{1}H-NMR spectra of the Asp235Ala variant are characteristic of a six-coordinate, high-spin heme iron(III) in which the sixth ligand is presumably provided by a water molecule. The heme methyl resonances exhibit a smaller chemical shift than those in the wild-type enzyme. This finding could reflect the fact that HS is hexaccordinate while wild-type enzyme is five-coordinate under the same conditions. Alternatively, the species in fast equilibrium with HS may be a low-spin, hexacoordinate iron (III) form so that the observed chemical shifts are an average of the chemical shifts for the two species that are in equilibrium.

At higher pH values, the iron converts to LS1 with a process that is slow on the NMR time scale. The conformational change implied by this observation is in agreement with the interpretation of spectrophotometric pH titrations reported for the Asp235Asn variant (Vitello et al., 1992). The electronic and ^{1}H-NMR spectra of LS1 are very similar to those of hydroxide-ligated metmyoglobin (Smulevich et al., 1991; Krishnamoorthi et al., 1984) and suggest that the sixth ligand in LS1 is a hydroxide ion that forms by the deprotonation of the water molecule bound to the iron in the low-pH form of Asp235Ala-CcP. The anti-Curie behavior of the paramagnetically shifted resonances of LS1, which indicates the partial low-spin nature of this species, provides additional support for this hypothesis. Hydroxide complexes of ferriheme proteins, like hydroxide-bound metmyoglobin which forms by the titration of the water molecule bound to the heme iron in met-aquomyoglobin with an apparent pK_a of 8–9 (Antonini & Brunori, 1971), exist generally as mixed-spin species. The presence of a positively charged residue (Arg48) and generally more polar residues in the distal cavity of CcP drastically reduces the pK_a of the metal-bound water molecule, as previously reported for HCA III (Bertini et al., 1985). The properties of this water molecule are also affected by the strength of the proximal iron ligand: a stronger proximal ligand favors the H_2O form with respect to OH^-.

Significantly, for wild-type CcP, which has an axial ligand with more histidinate character, a high/low-spin transition has been reported only above pH 8. In the case of the Asp235Asn variant, where the possibility of hydrogen-bond formation with His175 is not completely eliminated, the pK_a

for the high-spin to low-spin transition determined by electronic spectroscopy is slightly lower in nitrate (4.4) than in phosphate (5.0) (Vitello at al., 1992). On the other hand, analysis of this same equilibrium in nitrate by NMR spectroscopy was consistent with $pK_a \sim 6$ (Satterlee et al., 1990). This apparent discrepancy does not occur in the results reported here for the Asp235Ala variant, as both methods indicate a pK_a of ~ 5. Deprotonation of the distal water molecule must be accompanied by a significant conformational rearrangement in the distal heme pocket that probably involves Arg48 and adjacent water molecules. It has been shown that Arg48 moves toward the exterior of the pocket when C*c*P binds neutral ligands, while it moves toward the interior when anionic ligands bind. This movement of the Arg48 side chain, which can be as great as 2.5 Å in the fluoride complex of C*c*P, has been interpreted in terms of electrostatic and hydrogen-bonding interactions (Edwards & Poulos, 1990).

Increasing the pH further, LS1 converts into a new low-spin species, LS2, which probably involves the distal histidyl residue. Indeed, it has been shown that the variant in which this residue has been replaced by Ile does not give rise to any species similar to LS2 (Smulevich et al., 1991). The LS1 $\rightleftharpoons$ LS2 transition could represent the deprotonation of the distal histidine. It has previously been suggested on the basis of electronic and resonance Raman spectroscopy (Smulevich et al., 1991) that this transition involves the direct coordination of the distal histidine to the heme iron with the formation of a bis-histidine coordination environment. An alternative possibility is that the LS1 $\rightleftharpoons$ LS2 transition involves the disruption of the hydrogen bond between the distal histidine and the iron-bound hydroxyl group. This hypothesis is also consistent with the decrease in pK_{a2} observed with increasing temperature: at higher temperature, the hydrogen bond breaks more easily and, therefore, deprotonation is easier.

The calculated pK_a values for all the observed pH transitions in Asp235Ala-C*c*P are lower in nitrate-containing buffers than in phosphate buffers, indicating the existence of a specific anion effect. This observation can be explained only if nitrate and/or phosphate binds to the enzyme at a site that is probably near the heme pocket. A similar phenomenon has been reported for the Asp235Asn variant (Vitello et al., 1992). From the data currently available, it is not possible to establish which anion binds preferentially to the enzyme or which one is responsible for the observed changes in its behavior in different buffers. If nitrate binds, it apparently stabilizes those species that appear at higher pH. Alternatively, if phosphate binds, it stabilizes the low-pH forms of the enzyme.

Unfortunately, EPR spectroscopy cannot assist in the characterization of the axial ligation in these three forms of the variant enzyme because the EPR spectrum of the variant obtained at 4.2 K is that of a high-spin Fe(III) system over the pH range 5.5–8. Presumably, the equilibria in question are sufficiently temperature dependent that at the temperatures required for EPR spectroscopy, the protein coverts entirely to the high-spin form characteristic of the resting wild-type enzyme.

Functional Consequences of Replacing Asp235 with Ala. The steady-state activity of the Asp235Ala variant is 3 orders of magnitude smaller than that of the wild-type enzyme at all values of pH studied, while the pH dependencies of the two forms of the enzyme are very similar. This considerable reduction in activity presumably does not arise from inefficient production of compound I. Significantly, Vitello et al. (1992) have reported that the reactivity of the Asp235Asn variant with H_2O_2 is only slightly lower than that of the wild-type enzyme, and our preliminary results for the Asp235Ala variant are consistent with this finding (Ferrer, unpublished). It is unlikely that the stability of the cytochrome *c*–cytochrome *c* peroxidase complex is significantly affected by the Asp235Ala substitution because residue 235 is located internally and should not influence the cytochrome-binding site on the surface of the peroxidase. At present, it seems most likely that the great decrease in activity that results from replacing Asp235 with Ala arises from a reduction in the rate of intramolecular electron transfer from ferrocytochrome *c* to the oxidized peroxidase. The recent implication of Trp191 in this electron-transfer pathway (Pelletier & Kraut, 1992) combined with the reorientation of Trp191 on replacement of Asp235 with Ala (Goodin & McRee, 1993) provides circumstantial support for this suggestion.

Effects of the Asp235Ala Substitution on the Proximal Histidine. The ^{1}H-NMR spectra of heme protein cyanide-bound derivatives have been used in previous studies to characterize the properties of the proximal histidine. Upon binding of cyanide to the Asp235Ala variant, a single species is obtained at room temperature, and there is no evidence of equilibria of the type observed in the absence of cyanide. Structurally, elimination of the hydrogen bond between His175 and Asp235 could permit increased rotational freedom of the proximal histidine in the Asp235Ala variant. However, with the unambiguous assignment of the 8-CH_3 resonance by specific deuteration, it appears that the plane of the proximal histidine remains aligned along the axis connecting the nitrogen atoms of pyrroles I and III as in the wild-type protein and as found in the X-ray crystallographic structure of the Asp235Ala variant (Goodin & McRee, 1993). The chemical shifts of the proximal His protons in the cyanide derivatives of myoglobin and a series of peroxidases have been found to be phenomenologically related to the reduction potentials of the Fe^{3+}/Fe^{2+} couple of the noninhibited proteins (Banci et al., 1991b, 1993). This fact is not surprising insofar as the contact contribution of the hyperfine shift is related to the strength of the iron–His bond: the greater the donation from the proximal ligand to the iron, the lower the reduction potential and the greater the contact contribution of the parmagnetically induced shift.

The chemical shifts of the Hϵ1 and Hδ2 protons of the proximal histidine in the present variant (–9.7 and 14.6 ppm, respectively) are similar to those observed for LiP-CN^- (–9.0, 13.3; Banci et al., 1991b) and MnP–CN^- (–11.8, 20.3; Banci et al., 1992) and are distinctly different from those observed for HRP-CN^- (–29.9, 23.1; Thanabal et al., 1987b) and C*c*P-CN^- (–20.6, 15.8; Banci et al., 1991a). The current spectroscopic results combined with the reported reduction potential of the Asp235Ala variant (Goodin & McRee, 1993) are consistent with the previous conclusion (Banci et al., 1993) that decreasing the strength of the hydrogen bond to the proximal His ligand decreases the strength of the His–Fe bond and results in an increase in the Fe^{3+}/Fe^{2+} reduction potential. This potential is also influenced by electrostatic effects of charged groups in the protein on the heme iron. We note that in the present variant, the net electrostatic charge of the protein is changed by 1 (from –14 to –13) by elimination of the negative charge on Asp235.

A similar trend has been observed for the ^{15}N shifts of the bound cyanide anion in the series HRP (576 ppm), C*c*P (587 ppm), LiP (608 ppm), MnP (639 ppm) (Banci et al., 1993), and C*c*P-Asp235Ala (689 ppm), reflecting mainly the donor strength of the proximal histidyl ligand. On the other hand, the difference between the ^{15}N shift of bound CN^- in the

Asp235Ala variant and in metmyoglobin (930 ppm), both lacking the hydrogen bond between the proximal histidyl ligand and the aspartyl residue, must be attributable to distal contributions. Differences between the distal heme pockets of these two proteins also affect the ^1H hyperfine shifts of the proximal histidine. Indeed, the chemical shifts of Hϵ1 and Hδ2 of the proximal His residue in metmyoglobin are different from those of all peroxidases studied, including the Asp235Ala variant.

CONCLUDING REMARKS

From the present studies of the Asp235Ala variant, we conclude the following: (i) the pH-dependent properties of the distal cavity are strongly affected by features of the proximal iron ligand; (ii) the dependence of activity on pH is not affected by the unusual response of the Asp235Ala variant to changes in pH; (iii) the major role of Asp235 on the catalytic activity of the enzyme may be to maintain Trp191 in the correct orientation (through hydrogen bonding) for efficient electron transfer within the CcP–cytochrome *c* complex; and (iv) the Fe^{3+}/Fe^{2+} reduction potential of peroxidases is strongly dependent on the electronic properties of the proximal ligand.

REFERENCES

Antonini, E., & Brunori, M. (1971) *Hemoglobin and Myoglobin and Their Reactions with Ligands*, pp 47–48, North-Holland Publishing Co., Amsterdam.

Aue, W. P., Bartholdi, E., & Ernst, R. R. (1976) *J. Chem. Phys. 64*, 2229–2246.

Banci, L., Bertini, I., Luchinat, C., Piccioli, M., Scozzafava, A., & Turano, P. (1989) *Inorg. Chem. 28*, 4650–4656.

Banci, L., Bertini, I., Turano, P., Ferrer, J. C., & Mauk, A. G. (1991a) *Inorg. Chem. 30*, 4510–4516.

Banci, L., Bertini, L., Turano, P., Tien, M., & Kirk, T. K. (1991b) *Proc. Natl. Acad. Sci. U.S.A. 88*, 6956–6960.

Banci, L., Bertini, L., Pease, E. A., Tien, M., & Turano, P. (1992) *Biochemistry 31*, 10009–10017.

Banci, L., Bertini, I., Kuan, I.-C., Tien, M., Turano, P., & Vila, A. J. (1993) *Biochemistry 32*, 13483–13489.

Banci, L., Bertini, I., & Luchinat, C. *Methods Enzymol 239* (in press).

Behere, D. V., Gonzalez-Vergara, E., & Goff, H. M. (1985) *Biochem. Biophys. Acta 832*, 319–325.

Belton, P. S., Cox, I. J., & Harris, R. K. (1985) *J. Chem. Soc. Faraday Trans. 2*, 81, 63–75.

Bertini, I., & Luchinat, C. (1986) *NMR of Paramagnetic Molecules in Biological Systems*, Benjamin/Cummings, Menlo Park, CA.

Bertini, I., Dei, A., Luchinat, C., & Monnanni, R. (1985) *Inorg. Chem. 24*, 301–304.

Bertini, I., Capozzi, F., Luchinat, C., & Turano, P. (1991) *J. Magn. Reson. 95*, 244–252.

Bertini, I., Turano, P., & Vila, A. J. (1993a) *Chem. Rev. 93*, 2833–2932.

Bertini, I., Luchinat, C., & Tarchi, D. (1993b) *Chem. Phys. Lett. 203*, 445–449.

Blumberg, W. E., Peisach, J., Wittenberg, B. A., & Wittenberg, J. B. (1968) *J. Biol. Chem. 243*, 1854–1862.

Bosshard, H. R., & Yonetani, T. (1990) in *Peroxidases in Chemistry and Biology* (Everse, J., Everse, K. E., & Grisham, M. B., Eds.) Vols. 1 and 2, CRC Press, Boca Raton, FL.

Dasgupta, S., Rousseau, D. L., Anni, H., & Yonetani, T. (1989) *J. Biol. Chem. 264*, 654–662.

De Duve, C, (1948) *Acta Chem. Scand. 2*, 264.

de Ropp, J. S., La Mar, G. N., Smith, K. M., & Langry, K. C. (1984) *J. Am. Chem. Soc. 106*, 4438–4444.

de Ropp, J. S., La Mar, G. N., Wariishi, H., & Gold, M. M. (1991) *J. Biol. Chem. 266*, 15001–15009.

Edwards, S. L., & Poulos, T. L. (1990) *J. Biol. Chem. 265*, 2588–2595.

Edwards, S. L., Raag, R., Wariishi, H., Gold, M. H., & Poulos, T. L. (1993) *Proc. Natl. Acad. Sci. U.S.A. 90*, 750–754.

Erman, J. E., Vitello, L. B., Mauro, J. M., & Kraut, J. (1989) *Biochemistry 28*, 7992–7995.

Finzel, B. C., Poulos, T. L., & Kraut, J. (1984) *J. Biol. Chem. 257*, 13027–13036.

Fishel, L. A., Villafrance, J. E., Mauro, J. M., & Kraut, J. (1987) *Biochemistry 26*, 351–360.

Fitzgerald, M. M., McRee, D. E., Churchill, J. J., & Goodin, D. B. (in preparation).

Golding, R. M., Pascual, R. O., & Vrbancich, J. (1976) *J. Mol. Phys. 31*, 731–735.

Goodin, D. B., & McRee, D. E. (1993) *Biochemistry 32*, 3313–3324.

Goodin, D. B., Mauk, A. G., & Smith, M. (1987) *J. Biol. Chem. 262*, 7719–7724.

Goodin, D. B., Davidson, M. G., Roe, J. A., Mauk, A. G., & Smith, M. (1991) *Biochemistry 30*, 4953–4962.

Hager, L. P., Doubek, D. L., Silverstein, R. M., Hargis, J. H., & Martin, J. C. (1972) *J. Am. Chem. Soc. 94*, 4364–4366.

Hibler, D. W., Stolowich, N. J., Reynolds, M. A., Gerlt, J. A., Wilde, J. A., & Bolton, P. H. (1987) *Biochemistry 26*, 6278–6286.

Hockman, J., & Kellerhalls, H. P. (1980) *J. Magn. Reson. 38*, 23–39.

Hori, H. (1971) *Biochim. Biophys. Acta 251*, 227–235.

Inubushi, T., & Becker, E. D. (1983) *J. Magn. Reson. 51*, 128–133.

Jordi, H. C., & Erman, J. E. (1974) *Biochemistry 13*, 3734–3741.

Kang, D. S., & Erman, J. E. (1982) *J. Biol. Chem. 257*, 12775–12779.

Kaput, J., Goltz, S., & Blobel, G. (1982) *J. Biol. Chem. 257*, 15054–15058.

Kolthoff, I. M., & Belcher, R. (1957) *Volumetric Analysis*, Vol. III, pp 75–76, Interscience, New York.

Krishnamoorthi, R., La Mar, G. N., Mizukami, H., & Romero, A. (1984) *J. Biol. Chem. 259*, 265–270.

LaMar, G. N., & Walker, F. A. (1979) in *The Porphyrins Part IV-B* (Dolphin, D., Ed.) pp 61–157, Academic Press, New York.

La Mar, G. N., Horrocks, J. R., W. D., & Holm, R. H., Eds. (1973) *NMR of Paramagnetic Molecules*, Academic Press, New York.

La Mar, G. N., de Ropp, J. S., Chako, V. P., Satterlee, J. D., & Erman, J. E. (1982) *Biochim. Biophys. Acta 708*, 317–325.

Macura, S., Wüthrich, K., & Ernst, R. R. (1982) *J. Magn. Reson. 47*, 351–357.

Margoliash, E., & Frohwirt, N. (1959) *Biochem. J. 71*, 570–572.

Marion, D., & Wüthrich, K. (1983) *Biochim. Biophys. Res. Commun. 113*, 962–974.

Morishima, I., & Inubushi, T. (1977) *J. Chem. Soc., Chem. Commun.* 616–617.

Morishima, I., & Inubushi, T. (1978) *J. Am. Chem. Soc. 100*, 3568–3574.

Morishima, I., Inubushi, T., Neya, S., Ogawa, S., & Yonezawa, T. (1977) *Biochem. Biophys. Res. Commun. 78*, 739–746.

Pelletier, H., & Kraut, J. (1992) *Science 258*, 1748–1755.

Piontek, K., Glumoff, T., & Winterhalter, K. (1993) *FEBS Lett. 315*, 119–124.

Poulos, T. L., & Kraut, J. (1980) *J. Biol. Chem. 255*, 10322–10330.

Poulos, T. L., Edwards, S. L., Wariishi, H., & Gold, M. H. (1993) *J. Biol. Chem. 268*, 4429–4440.

Rafferty, S. P., Pearce, L. L., Barker, P. D., Guillemette, J. G., Kay, C. M., Smith, M., & Mauk, A. G. (1990) *Biochemistry 29*, 9365–9369.

Satterlee, J. D., & Erman, J. E. (1991) *Biochemistry 27*, 4398–4405.

Satterlee, J. D., Erman, J. E., La Mar, G. N., Smith, K. M., & Langry, K. C. (1983) *J. Am. Chem. Soc. 105*, 2099–2104.
Satterlee, J. D., Erman, J. E., Mauro, M. J., & Kraut, J. (1990) *Biochemistry 29*, 8797–8804.
Satterlee, J. D., Russel, D. J., & Erman, J. E. (1991) *Biochemistry 30*, 9072–9077.
Shiro, Y., Iizuka, T., Makino, R., Ishimura, Y., & Morishima, I. (1989) *J. Am. Chem. Soc. 111*, 7707–7711.
Shulman, G., Glarum, S. H., & Karplus, M., (1971) *J. Mol. Biol. 57*, 93–115.
Sivaraja, M., Goodin, D. B., Smith, M., & Hoffman, B. M. (1989) *Science 245*, 738–740.
Smith, K. M., Miura, M., Morris, I. K. (1986) *J. Org. Chem. 51*, 4660–4667.
Smulevich, G., Mauro, J. M., Fishel, L. A., English, A. M., Kraut, J., & Spiro, T. G. (1988) *Biochemistry 27*, 5477–5485.
Smulevich, G., Wang, Y., Mauro, J. M., Wang, J., Fishel, L. A., Kraut, J., & Spiro, T. G. (1990) *Biochemistry 29*, 7174–7180.
Smulevich, G., Miller, M. A., Kraut, J., & Spiro, T. G. (1991) *Biochemistry 30*, 9546–9558.
Studier, F. W., Rosenberg, A. H., Dunn, J. J., & Dubendorff, J. W. (1990) *Methods Enzymol. 185*, 60–89.
Thanabal, V., de Ropp, J. S., & La Mar, G. N. (1986) *J. Am. Chem. Soc. 108*, 4244–4245.
Thanabal, V., de Ropp, J. S., & La Mar, G. N. (1987a) *J. Am. Chem. Soc. 109*, 265–272.
Thanabal, V., de Ropp, J. S., & La Mar, G. N. (1987b) *J. Am. Chem. Soc. 109*, 7516–7525.
Thanabal, V., La Mar, G. N., & de Ropp, J. S. (1988) *Biochemistry 27*, 5400–5407.
Vitello, L. B., Erman, J. E., Miller, M. A., Mauro, J. M., & Kraut, J. (1992) *Biochemistry 31*, 11524–11535.
Yonetani, T. (1967) *J. Biol. Chem. 242*, 5008–5013.
Wang, J., Mauro, M., Edwards, S. L., Oatley, S. J., Fishel, L. A., Ashford, V. A., Xuong, N., & Kraut, J. (1990) *Biochemistry 29*, 7160–7173.
Wittenberg, B. A., Kampa, L., Wittenberg, J. G., Blumber, W. E., & Peisach, J. (1968) *J. Biol. Chem. 243*, 1863–1870.
Yonetani, T., & Ray, G. S. (1965) *J. Biol. Chem. 240*, 4503–4508.
Yonetani, T., & Anni, H. (1987) *J. Biol. Chem. 262*, 9547–9554.
Yu, L. P., La Mar, G. N., & Rajanathnam, K. (1990) *J. Am. Chem. Soc. 112*, 9527–9534.